university of groningen
faculty of science and engineering
mathematics and applied mathematics
physics and applied physics

Elliptical billiard systems and chaotic micro-lasers

Bachelor's Project Mathematics & Physics

July 2020

Student: R.W.H. Zwiers

Mathematics supervisor: Prof. H. Waalkens

Physics supervisor: Prof. G. Palasantzas

Abstract

This paper will discuss billiard systems, especially elliptical ones, with the main focus on finding the mean minimal action function α of these systems. This function plays a crucial role in understanding different rigidity phenomena that appear in the study of convex billiards and is also widely used in Aubrey-Mather theory. Billiard systems in general will be discussed before deriving the α function. These results will then be illustrated using an example of circular billiards. Then the elliptical billiard systems will be discussed in detail, the mean minimal action α will be derived and results will be compared with the circular billiards. Furthermore, chaotic micro-lasers will be covered, what they are, and how they are related to billiard systems.

Contents

1 Introduction

Billiard systems are a well-known subject in the area of physics and mathematics. They are dynamical systems in which a particle switches between free motion and reflections from a boundary. This concept can be used for quantum systems, as well as classical systems, and for studying the classical limit of quantum mechanics using semi-classical tools. These systems can capture the complexity of Hamiltonian systems without integrating the equations of motion and can be used to model real-world systems.

In this paper, billiard systems will be discussed, with the main goal to determine the mean minimal action function α in the case of an elliptical billiard system.

The first part of the paper will start by explaining the general notion of billiard systems. Then the existence of so-called caustics in these systems will be discussed. Then the mean minimal action function α will be introduced and be discussed in some detail. To give some idea about these parts, an example of a circular billiard will be given.

The second part of the paper will be covering the derivation of the mean minimal action function α for the case of the elliptical billiard system. This will be done by first introducing the billiard family, denoting the Hamiltonian of the system, and use this to find the actions and winding number. Then these results will be used to derive α and it will be compared to the circular case.

The last part of the paper will be about an application of the results from the first two parts. It will cover the so-called chaotic micro-lasers. First, it will be explained what they are and where they are used. Then the physics of the chaotic micro-lasers will be discussed in detail, and the connection to the billiard systems will be looked at.

2 Billiards Systems

Before looking for the mean minimal action in a billiard system, first billiard systems need to be discussed in general. A billiard system is a dynamical system in which a particle alternates between free motion and specular reflections from a boundary. These billiard systems are Hamiltonian idealizations of the game of billiards, but the region contained by the boundary can have shapes other than rectangular, like circular and elliptical, and they can even be multidimensional.

The motion of a particle in billiard systems can be seen as a straight line between reflections with the boundary. All reflections are specular, which means that the angle of incidence is equal to the angle of reflection, see Figure 1. Furthermore, the energy of the particle is conserved during reflections. This sequence of reflections is described by the billiard map, and it completely characterizes the motion of the particle. This billiard map transforms the coordinates and incident angle of the point of reflection into the coordinates and the incident angle at the point of the next reflection from the boundary.

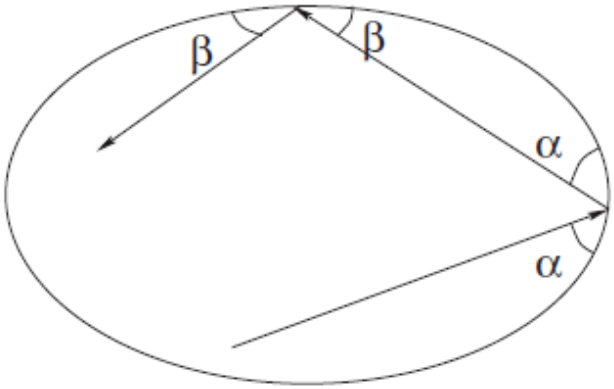

Figure 1: Billiard reflections.

Billiard systems are Hamiltonian systems, which have a potential $V(q)$ that is equal to zero within a domain, which will be denoted by Ω, and infinity outside. The dynamics of the billiard systems are completely defined by the shape of its boundary $\partial\Omega$. It captures all possible behaviors of Hamiltonian systems, from integrable to completely chaotic ones. One has to note, even though the dynamics is relatively simple, without the difficulties of integrating the equations of motion, computation of the billiard map can still be rather difficult.

Both classical and quantum billiard systems have several applications in physics, where they are used to model many real-world systems, for example ray-optics, lasers, or the study of quantum chaos [12]. One example that will be covered in this paper is the case of chaotic micro-lasers. Billiard systems are thus widely used as

physical models. This is because when there is little disorder or noise, the movement of for example particles like electrons or light rays, is rather similar to the movement of the point-particles in billiards. Furthermore, since the particle collisions in a billiard system conserve energy, it can be seen as a reflection of the conservation of energy in Hamiltonian mechanics.

In this paper, the focus will be on billiard systems for the case of convex boundaries, especially the case when the boundary is elliptical. The motion in these systems is sometimes called "whispering gallery motion". This name is due to the effect that is usually called a "whispering gallery". When waves get reflected and travel along a convex wall, they will always stay close to it. This phenomenon was first explained for the case of St Paul's Cathedral by Lord Rayleigh [9]. Furthermore, there is the Birkhoff-Poritsky conjecture [8], which says that the ellipse is the only integrable smooth convex billiard, where the circle is the special case of an ellipse. Whenever a billiard system is integrable, the corresponding quantum system is completely solvable.

Taking a billiard system with a strictly convex boundary, suppose there is a smooth, strictly convex domain in $\mathbb{R}^2$, denoted by Ω. Then a closed geodesic in this domain is a broken geodesic in $\mathbb{R}^2$, which is reflected at the boundary according to the law that the angle of reflection is equal to the angle of incidence. To distinguish these geodesics in the system, to each geodesic one can assign a rotation number, which will be denoted by ω and is given by

$$\omega = \frac{m}{n} = \frac{\text{winding number}}{\text{number of reflections}} \in (0, \frac{1}{2}].$$

Here, the winding number is defined by fixing the positive orientation of $\partial\Omega$ and picking any corner point of the closed geodesic on $\partial\Omega$. Then one follows the geodesic and measures how many times it goes around $\partial\Omega$ until it comes back to the starting point.

Furthermore, closed geodesics maximize the length of the perimeter of the inscribed n-gons in Ω with winding number m. The billiard map associated to Ω is then denoted by

$$\begin{aligned} \phi : S^1 \times (0, \pi) &\to S^1 \times (0, \pi), \\ (s_1, \Phi_1) &\mapsto (s_2, \Phi_2) \end{aligned} \tag{1}$$

where (s, Φ)=(arclength on $\partial\Omega$, angle with the positive tangent of $\partial\Omega$).

Let

$$h(s, s') = -|P(s) - P(s')|$$

denote the negative Euclidean distance between two reflection points on $\partial\Omega$.

Then one has that

$$\partial_1 h(s_0, s_1) = \cos(\Phi_0) \text{ and } \partial_2 h(s_0, s_1) = -\cos(\Phi_0).$$

In other words, in new coordinates

$$(x, y) = (s, -cos(\Phi)$$

one has

$$y_1 dx_1 - y_0 dx_0 = dh(x_0, x_1). \tag{2}$$

Then ϕ is exact symplectic [11] on $S^1 \times (-1, 1)$ and has generating function being the negative Euclidean distance between two points on $\partial\Omega$ and is denoted by

$$h(s, s') = -|P(s) - P(s')|. \tag{3}$$

If a billiard system is integrable, then by the Liouville-Arnold Theorem [1] there exists a canonical transformation to action-angle coordinates. Here the transformed Hamiltonian is dependent only upon the action coordinates and the angle coordinates evolve linearly in time. Then for such an integrable system in $\mathbb{R}^2$, the motion of the billiard system is confined in a two-dimensional manifold, called a 2-torus, as can be seen in Figure 2. Here I_1 and I_2 are the actions associated to the system.

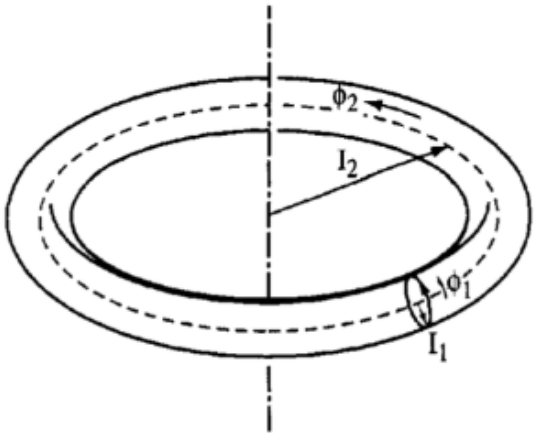

Figure 2: In $\mathbb{R}^2$, integrable motion is confined within a 2-torus.

One more characteristic of the billiard system is the so-called caustic, as can be seen in Figure 3. A convex caustic **c** is a closed convex C^l-curve in the interior of Ω with the property that every trajectory tangent to c stays tangent after each reflection. The existence of these caustics is not proved in this paper, but for the proof one can refer to the paper by Lazutkin [5].

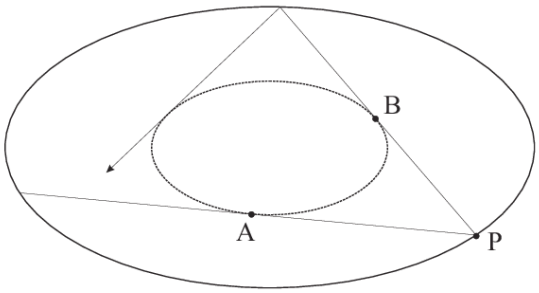

Figure 3: A convex caustic

Given such a convex caustic $\mathbf{c}$, the following parameters can be defined:

1. its rotation number $\omega \in (0, \frac{1}{2})$;
2. its length $\mathrm{L}(\mathbf{c})$;
3. its Lazutkin parameter $Q(\mathbf{c}) = |A - P| + |P - B| - |\widehat{AB}|$, with $A, B \in \mathbf{c}$ and $P \in \partial\Omega$ as in Figure 1. Here $|\widehat{AB}|$ denotes the length of the caustics part from A to B, where the caustic is oriented according to the geodesics touching it.

If $\mathbf{c}$ is a caustic, then the Lazutkin parameter is well defined, i.e., it does not depend on the point $P \in \partial\Omega$ [5].

Now, the next goal will be to derive the so-called mean minimal action function α, especially for the case of an elliptical billiard system. This function is related to the maximal length of periodic orbits with a given rotation number, which are called marked length spectra. Furthermore, it plays a crucial role in understanding different rigidity phenomena that appear in the study of convex billiards. The mean minimal action α also contains several geometric parameters of Ω. Some of those are for example its diameter, its boundary length, and the parameters of the convex caustic. To be more precise, the mean minimal action associated to Ω is a strictly convex function

$$\alpha : [0, 1] \to \mathbb{R}$$

with convex conjugate

$$\alpha^* : [-1, 1] \to \mathbb{R}.$$

To find such a function, let us look again at the billiard map. The billiard map as defined in (1) is a monotone twist map on $S^1 \times (-1, 1)$ with twist interval $[\omega_-, \omega_+]$ [11]. Furthermore, it was noted that the billiard systems contain geodesics that maximize the perimeter. Maximizing length means minimizing the action, which is defined as the sum of the generating function h along the orbit. Using the results

from Aubry-Mather theory [2], there are minimal orbits of all rotation numbers. The mean minimal action can then be defined as

$$\alpha : [\omega_-, \omega_+] \to \mathbb{R}$$

by associating to ω the mean action of a minimal orbit (x_i, y_i) of rotation number ω

$$\alpha(\omega) = \lim_{N\to\infty} \frac{1}{N} \sum_{i=0}^{N-1} h(x_i, x_{i+1}). \tag{4}$$

Furthermore, its convex conjugate function

$$\alpha^* : [-1, 1] \to \mathbb{R}$$

is the Legendre transformation of α. The convex conjugate of a function is then a generalization of the Legendre transformation, which applies to non-convex functions. It is commonly used to go from Lagrangian to Hamiltonian dynamics. The convex conjugate is then defined by

$$\alpha^*(I) = \max_{\omega}[\omega I - \alpha(\omega)] \tag{5}$$

Since one has that α is continuous and is everywhere differentiable [6], equation (5) can also be written as

$$\alpha^*(I) = \left(I\omega - \alpha(\omega)\right)\big|_{\omega=(\alpha')^{-1}(I)}. \tag{6}$$

Now, let us look at the relation between this mean minimal action function and the geometric parameters of the convex caustic. If one has a convex caustic of rotation number ω denoted by c_ω, then one has that the length of the caustic is given by

$$L(c_\omega) = -\alpha'(\omega) \tag{7}$$

and its Lazutkin parameter is given by

$$Q(c_\omega) = \alpha^*(\alpha'(\omega)). \tag{8}$$

Furthermore, given such a convex caustic c_ω, one can reconstruct $\partial\Omega$ by wrapping a string of length $L(c_\omega) + Q(c_\omega)$ around c_ω, pulling it tight and going along c_ω.

To give an example of the derivation of the mean minimal action α for a billiard system, let us look at the following example of a circular billiard system.

Example: Take a circular billiard with perimeter 1 in $\mathbb{R}^2$. The whispering gallery motion in such a circular billiard can be seen in Figure 4.

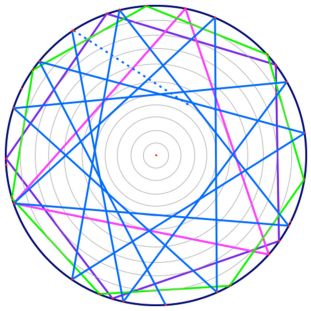

Figure 4: Whispering gallery motion for a circular billiard.

Furthermore, the billiard map is given by

$$(s_1, \phi_1) = (s_0 + \frac{\phi_0}{\pi}, \phi_0),$$

with generating function

$$h(s, s') = -\frac{1}{\pi} \sin \pi(s - s').$$

Since the whole space is covered by rotational invariant curves, the minimal action can be given by

$$\alpha(\omega) = -\frac{1}{\pi} \sin \pi\omega.$$

Furthermore, the derivative of α is given by

$$\alpha'(\omega) = -\cos(\pi\omega) \equiv I.$$

The convex conjugate α^* can be determined using the Legendre transform of α, yielding

$$\alpha^*(I) = \frac{1}{\pi}\Big(\arccos(-I) \cdot I + \sqrt{1 - I^2}\Big).$$

The graphs of these functions are plotted in Figure 5.

By equation (7), one has that the length of the caustic in this system is given by

$$L(c_\omega) = -\alpha'(\omega) = \cos(\pi\omega).$$

For $\omega = 0$ on has the sliding motion along the boundary, thus the length of the caustic should be 1. For $\omega = \frac{1}{2}$, one has the motion of the ball bouncing between two fixed points, thus the length of the caustic should be 0. For values of ω between 0 and $\frac{1}{2}$, the length will be between 0 and 1, hence $L(c_\omega) = \cos(\pi\omega)$ correctly describes the length of the caustic. Furthermore, by equation (8) the Lazutkin parameter is given by

$$Q(c_\omega) = \alpha^*(-\cos(\pi\omega)) = \alpha^*(I).$$

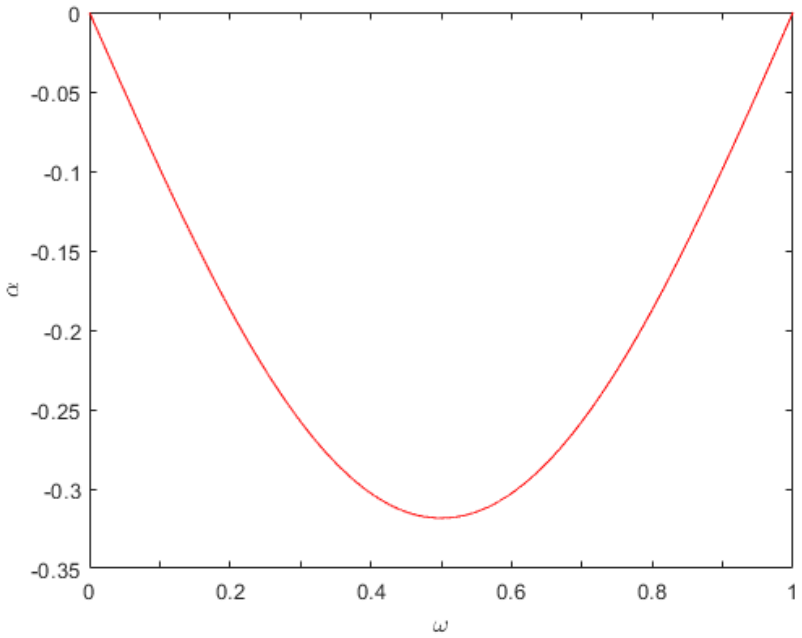

(a)

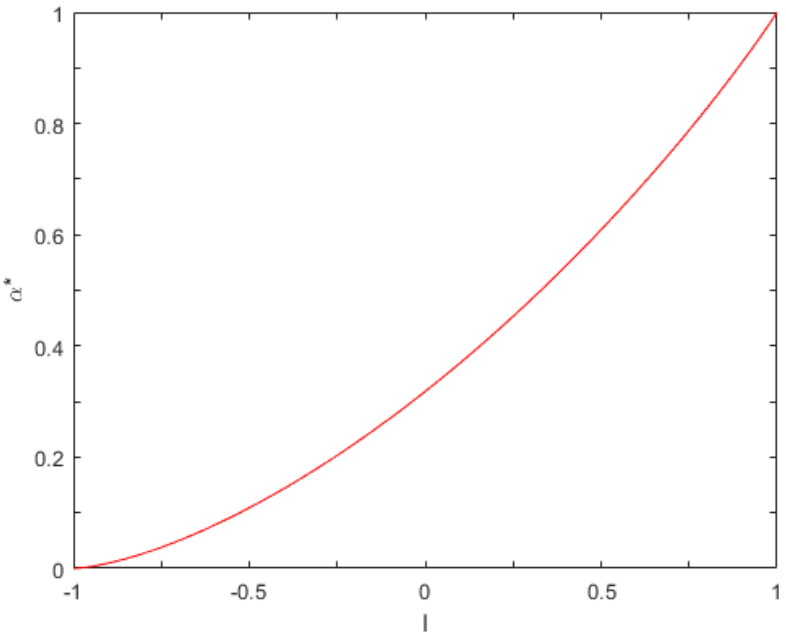

(b)

Figure 5: (a) α as a function of the winding number ω and (b) α^* as a function of the action I for circular billiards.

3 Elliptical Billiards

Normally, when deforming the circular billiard, one would destroy the 2-tori in the billiard system, and hence destroy the whispering gallery motion. However, in the special case of the elliptical billiard, some of these 2-tori remain intact, and the whispering gallery motion can again be observed. Thus, one can also obtain the minimal action function α for the elliptical billiard system.

To illustrate this fact, let one take the billiard family with boundary

$$x^2 + \frac{y^2}{1-a^2} = 1,$$

where $0 \leq a < 1$. Here, a is called the eccentricity of the ellipse and the foci of the ellipse are at $(x, y) = (\pm a, 0)$. This can then be written in terms of orthogonal coordinates (ξ, η), where $\xi =$ constant and $\eta =$ constant are sets of confocal ellipses and hyperbolas. Then the elliptic coordinate system can be denoted by

$$(x, y) = \Big(\frac{1}{a}\xi\eta, \pm\frac{1}{a}\sqrt{(\xi^2 - a^2)(a^2 - \eta^2)}\Big),$$

where $a \leq \xi \leq 1$ and $-a \leq \eta \leq a$. The Hamiltonian of this systems in terms the (ξ, η)-coordinates and corresponding momenta (p_ξ, p_η) is given by

$$H = \frac{1}{2}\frac{1}{\xi^2 - \eta^2}\Big((\xi^2 - \eta^2)p_\xi^2 + (a^2 - \eta^2)p_\eta^2\Big). \tag{9}$$

This Hamiltonian is only the product of the kinetic energy, since inside the boundary of a billiard system, the potential energy is zero. Furthermore, two types of reflection have to be considered. The first one is the reflection at the boundary $\xi = 1$, where p_ξ changes sign, and can be denoted by

$$(\xi, \eta, p_\xi, p_\eta) \to (\xi, \eta, -p_\xi, p_\eta). \tag{10}$$

The second one is the reflection at either $\xi = a$ or $\eta = \pm a$. In the case that $\xi = a$, one gets the same as in equation (10). For the case that $\eta = \pm a$, there is instead a change of sign of p_η, which can be denoted by

$$(\xi, \eta, p_\xi, p_\eta) \to (\xi, \eta, p_\xi, -p_\eta). \tag{11}$$

This system is integrable since the two coordinates (ξ, η) can be separated. This can be done by equating H to E and then multiplying by $\xi^2 - \eta^2$. Then, using a separation constant K, one gets the following equations

$$2E\xi^2 - (\xi^2 - a^2)p_\xi^2 = K \equiv 2E\kappa^2 \tag{12}$$

$$2E\eta^2 + (a^2 - \eta^2)p_\eta^2 = K \equiv 2E\kappa^2, \tag{13}$$

where κ^2 is the scaled constant of motion, which has allowed values $0 \leq \kappa^2 \leq 1$. This can easily be seen since $\kappa^2 > 0$ and by noting that for $\kappa^2 > 1$ one must have that p_ξ^2 or p_η^2 are negative to satisfy both equations, which is mathematically not possible.

Since the system is integrable, one has that the energy surface is foliated by invariant 2-tori, which are defined by the values of E and κ^2. One can characterize these tori by looking at the fundamental actions, which are defined by

$$I_j = \frac{1}{2\pi} \oint p dq, \tag{14}$$

where the integral is taken along fundamental paths on the tori.

Their intersections with the (ξ, p_ξ)- and (η, p_η)-plane can be found by solving equations (12) and (13) for the corresponding momenta. This yields the following

$$p_\xi^2 = 2E\frac{\xi^2 - \kappa^2}{\xi^2 - a^2} \tag{15}$$

$$p_\eta^2 = 2E\frac{\kappa^2 - \eta^2}{a^2 - \eta^2} \tag{16}$$

Using equations 15 and 16, one can construct the phase portraits in Figure 6.

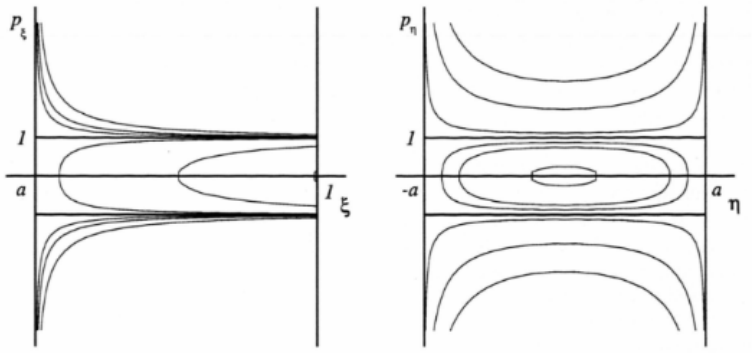

Figure 6: Phase portraits for the elliptical billiards. *Left*: Intersection of invariant 2-tori with (ξ, p_ξ)-plane. *Right*: Intersection of invariant 2-tori with (η, p_η)-plane.

From this figure, one can also see that there are two types of tori in this case, with a seperatix dividing them. For $\kappa^2 > a^2$, there is the whispering gallery motion seen before in the circular billiards. Here the geodesics avoid the region in the interior

of the ellipse, touching the boundary of this between consecutive reflections at the billiard boundary. In configuration space, the confocal ellipse $\xi = \kappa$ can be seen as an inner envelop, where the momentum p_ξ along a solution curve goes to zero and changes sign. The other type of tori is obtained when $\kappa^2 < a^2$, representing the so-called bouncing ball motion. Here, the geodesics always cross the x-axis between the foci, they are confined to the domain enclosed by the hyperbolas given by $\eta = \pm\kappa$. The motion of the whispering gallery and bouncing ball in configuration space can be seen in Figure 7, The special case when $\kappa^2 = 0$ represents the stable oscillation along the y-axis. The other special case, when $\kappa^2 = 1$ represents the sliding motion along the boundary. In the system, there is also a seperatix motion when $\kappa^2 = a^2$. The seperatix consists of the stable and unstable manifolds of the unstable periodic orbit. This unstable periodic orbit runs along the horizontal symmetry line which contains the two foci and the orbits in the stable/unstable manifolds alternately go through one of the two focus points between every two consecutive reflections. In this paper, only the whispering gallery motion will be discussed in detail.

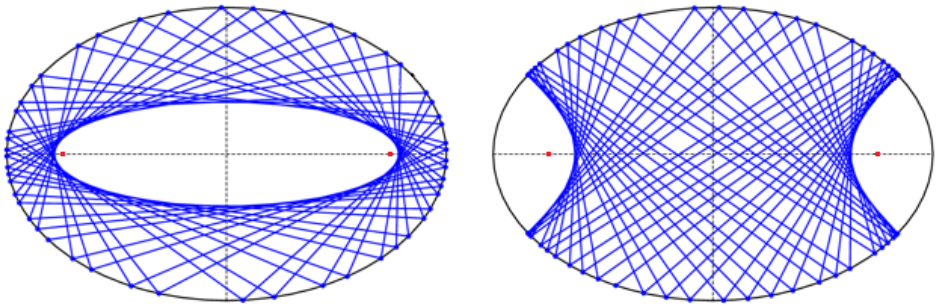

Figure 7: Motion in configuration space for elliptical billiards. *Left*: Whispering gallery. *Right*: Bouncing ball.

Knowing the types of motions in the elliptical billiard system, let us now look at the derivation of the actions. The actions for the whispering gallery motion can be found by using equations (12), (13), and (14) and both actions are scaled by energy. For the action related to ξ, one gets the following

$$\begin{aligned} I_1 = \frac{1}{\sqrt{2E}} I_\xi &= \frac{1}{2\pi} \oint \frac{p_\xi}{\sqrt{2E}} d\xi \\ &= \frac{2}{\pi} \int_\kappa^1 \sqrt{\frac{\xi^2 - \kappa^2}{\xi^2 - a^2}} d\xi \\ &= \frac{1}{\pi} \Big(\sin\phi - \kappa \mathcal{E}(\phi, \frac{a}{\kappa}) \Big) \end{aligned} \tag{17}$$

where $\sin^2\phi = \frac{1-\kappa^2}{1-a^2}$.

For the action related to η, one gets the following

$$\begin{aligned} I_2 = \frac{1}{\sqrt{2E}} I_\eta &= \frac{1}{2\pi} \oint \frac{p_\eta}{\sqrt{2E}} d\eta \\ &= \frac{2}{\pi} \int_0^a \sqrt{\frac{\kappa^2 - \eta^2}{a^2 - \eta^2}} d\eta \\ &= \frac{2\kappa}{\pi} \mathcal{E}(\frac{a}{\kappa}). \end{aligned} \tag{18}$$

Here, $\mathcal{E}(\frac{a}{\kappa})$ denotes the complete elliptic integral of first kind and $\mathcal{E}(\phi, \frac{a}{\kappa})$ denotes the incomplete elliptic integral of second kind, where ϕ is the amplitude and κ the modulus. Furthermore, the rotation number is

$$\omega = \frac{\omega_\eta}{\omega_\xi} = -\frac{I_\xi}{I_\eta}\bigg|_E = \frac{1}{2} \frac{\mathcal{F}(\phi, a/\kappa)}{\mathcal{K}(a/\kappa)}. \tag{19}$$

Having found the formulas for the actions and winding number, the next step will be to get the minimal action function α for the case of an elliptical billiard. To find α, one first has to find the generating function, which was defined to be the negative Euclidean distance between two consecutive reflection points. Let γ be a path between two consecutive reflection points in configuration space, with parametrization given by

$$t \mapsto \big(x(t), y(t)\big), \quad t \in [0, T],$$

where T is some parameter which will be sent to infinity. This parametrization is such that $\left(\frac{dx(t)}{dt}, \frac{dy(t)}{dt}\right) =: \vec{v}(t)$ has constant norm $||\vec{v}(t)|| =: \sqrt{\frac{2E}{m}}$. Then the length of γ can be computed in several steps. First one has

$$\begin{aligned} \int_\gamma ds &= \int_0^T \Big((\frac{dx}{dt})^2 + (\frac{dy}{dt})^2 \Big)^{\frac{1}{2}} dt \\ &= \int_0^T ||\vec{v}(t)|| dt \end{aligned} \tag{20}$$

since $\left(\frac{dx(t)}{dt}, \frac{dy(t)}{dt}\right) =: \vec{v}(t)$. Furthermore, since by definition $\vec{p}(t) = m\vec{v}(t)$ and $||p|| = \sqrt{2mE}$, one has

$$\begin{aligned} \int_0^T ||\vec{v}(t)|| dt &= \frac{1}{m} \int_0^T ||\vec{p}(t)|| dt \\ &= \frac{1}{m||p||} \int_0^T \vec{p}(t) \cdot \vec{p}(t) dt \\ &= \frac{1}{\sqrt{2mE}} \int_0^T \vec{p}(t) \cdot \vec{v}(t) dt \end{aligned} \tag{21}$$

Now, assume that $\tilde{\gamma}$ is a path in phase space different from the fundamental paths on the torus. Let $\beta = \vec{p}\cdot d\vec{q} = \sum_i p_i dq_i$ be the tautological 1-form with $d\beta = \sum_i dp_i \wedge dq_i$ being the a canonical 2-form. Then β is conserved under cotangent lifts of point transformations. Using this fact, one has that

$$\begin{aligned}\frac{1}{\sqrt{2mE}}\int_0^T \vec{p}(t)\cdot\vec{v}(t)dt &= \frac{1}{\sqrt{2mE}}\int_{\tilde{\gamma}} \vec{p}\cdot d\vec{q} \\ &= \frac{1}{\sqrt{2mE}}\int_{\tilde{\gamma}} p_\xi d\xi + p_\eta d\eta \\ &= \frac{1}{\sqrt{2mE}}\Big(\int_{\tilde{\gamma}} p_\xi d\xi + \int_{\tilde{\gamma}} p_\eta d\eta\Big)\end{aligned} \tag{22}$$

Since $\tilde{\gamma}$ is a path in phase space different from the fundamental paths on the 2-torus, it can be seen as a combination of those fundamental paths. One can also look at the 2-torus as a square, where the fundamental paths corresponding to ξ and η go horizontal and vertical respectively along the square. The path $\tilde{\gamma}$ can then be seen as a sloped line on the square, where instead of a reflection at $\partial\Omega$, the square is reflected and the particle will move straight into this mirror image. This can be seen in Figure 8.

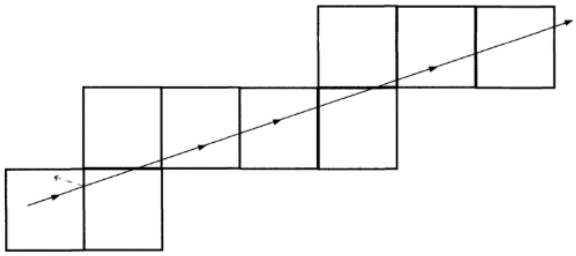

Figure 8: Unfolding a path on the 2-torus.

The slope can then be accounted for by multiplying vertically by the rotation number ω. Thus the path $\tilde{\gamma}$ can be seen as a combination of the fundamental paths. This allows us to do the integrals in equation (22) with respect to their corresponding fundamental path, where the integral relating to η needs to be multiplied by ω. One can then use equation (14), (17) and (18) and assuming $m = 1$ to get

$$\begin{aligned}\frac{1}{\sqrt{2mE}}\Big(\int_{\tilde{\gamma}} p_\xi d\xi + \int_{\tilde{\gamma}} p_\eta d\eta\Big) &= \frac{2\pi}{\sqrt{2mE}}(I_\xi + \omega I_\eta) \\ &= 2\pi(I_1 + \omega I_2)\end{aligned} \tag{23}$$

Combining (20), (21), (22) and (23), one has the following for the length of γ

$$\int_\gamma ds = 2\pi(I_1 + \omega I_2) \tag{24}$$

Now, as the generating function was defined as the negative Euclidean distance between two reflection points, it is computed to be

$$h = -2\pi(I_1 + \omega I_2) \tag{25}$$

Having found the generating function for the elliptical billiards, the mean minimal action α can be computed by using equation (4). This gives the following

$$\alpha(\omega) = -2\pi(I_1 + \omega I_2) \tag{26}$$

where ω, I_1, I_2 are given by equation (19), (17), (18) respectively. Furthermore, the derivative of α is given by

$$\alpha'(\omega) = -2\pi(I_1 + \omega \frac{dI_1}{d\omega} + \frac{dI_2}{d\omega}).$$

As ω, I_1 and I_2 are functions of the separation constant κ, applying the chain rule yields

$$\frac{d\omega}{d\kappa} = -\frac{d}{d\kappa}\frac{dI_1}{dI_2} = -\frac{d}{d\kappa}\frac{dI_1/\kappa}{dI_2/\kappa} = \frac{I_2' I_1" - I_2" I_1'}{(I_1)^2}.$$

Using this in combination with the previous found derivative yields

$$\alpha'(\omega) = -2\pi I_1 \equiv I. \tag{27}$$

Furthermore, the convex conjugate of α, denoted by α^* can be determined using the Legendre transform of α. This then yields the following

$$\alpha^*(I) \equiv I\omega - \alpha = 2\pi I_2. \tag{28}$$

To compare these results with the example of a circular billiard, before plotting the function $\alpha(\omega)$ and $\alpha^*(I)$, a scaling will be introduced, such that the perimeter of the elliptical billiards becomes unity. This is done by taking $(x, y) \to (x/c, y/c)$ where $c = 8\mathcal{E}(a)$ is the perimeter of the original billiard boundary. The scaled actions are then given by I_1/c and I_2/c. The resulting figures for $\alpha(\omega)$ and $\alpha^*(I)$ are shown in Figure 9. It can be seen that for $a = 0$, indeed the same result as for the circular billiard in Figure 5 is obtained.

Having found the mean minimal action α, one can also say something about the geometric properties of the elliptic billiard and its caustic. According to equation (7), the length of the caustic should be equal to $-\alpha'(\omega) = 2\pi I_1$. The caustic in this case is an ellipse that is given by the elliptic coordinate line denoted by $\xi = \kappa$. Its length is $L(c) = 4\kappa\mathcal{E}(\frac{a}{\kappa})$, which is indeed equal to $2\pi I_1$. The action I_1 can thus be described as the length of the caustic, up to a factor of 2π. Furthermore, by equation (8), the Lazutkin parameter is given by $Q(c_\omega) = \alpha^*(-2\pi I_1) = \alpha^*(I)$.

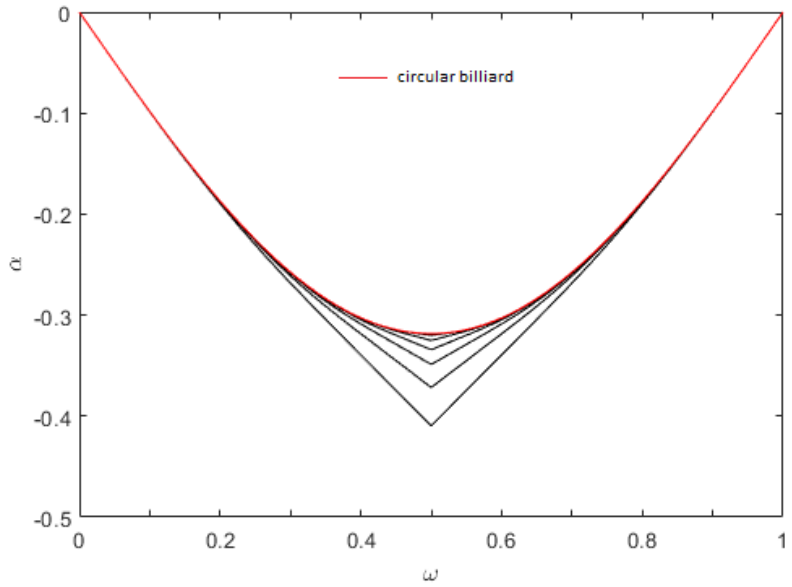

(a)

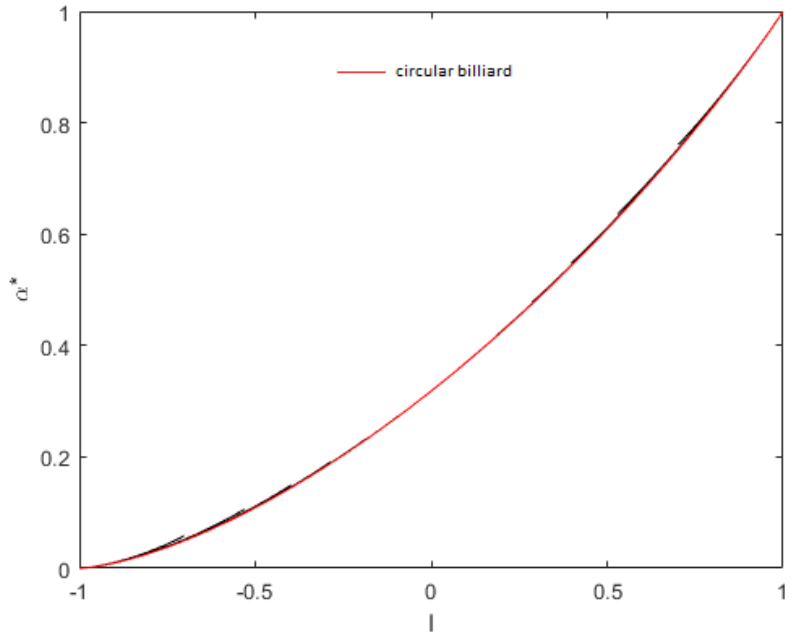

(b)

Figure 9: (a) α as a function of the winding number ω and (b) α^* as a function of the action I for elliptic billiards with eccentricity n/7, n=0,1,2,3,4,5,6, where n=0 is the circular billiard.

4 Chaotic Micro-lasers

One application of the billiard systems covered up till now are so-called chaotic micro-lasers. In these lasers, one can see similar motion for light to the whispering gallery motion in the billiard systems

Starting in the mid 1990s, chaotic micro-lasers have been established as an alternative to the conventional and well-known Fabry-Perot lasers, in the course of the ongoing miniaturization of devices. Chaotic micro-lasers are typically realized as so-called micro-cavity lasers. These are essentially planar systems, so the third dimension can be neglected, of a slightly deformed disk shape, which can be seen in Figure 10.

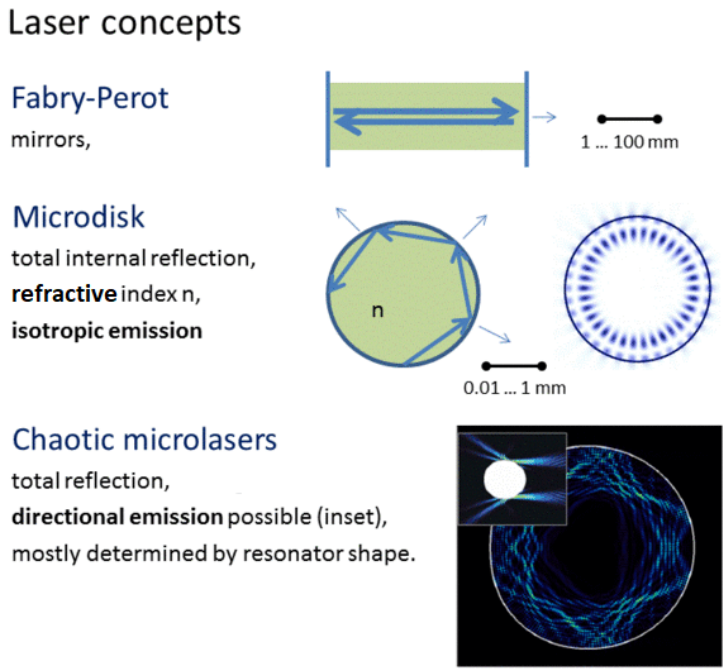

Figure 10: Different types of lasers.

Micro-cavity lasers are a new way to look at the fields of chaos and quantum chaos, because they basically represent open two-dimensional billiards systems. Therefore, the theoretical description of chaotic micro-lasers turns out to be very closely related to the fields of dynamical systems. As in micro-disk lasers light may escape by means of diffraction, they can be seen as intrinsically open systems. Furthermore, the hard-wall case is only reached in the limit of an (infinitely) large refractive index. This can then be seen as a closed billiard system, as studied in this paper.

These chaotic micro-lasers thus exploit the total internal reflection of light to achieve mirror reflectivity. Micro-disk lasers are a class of lasers that are based on circularly symmetric resonators, which lase on whispering gallery modes of the electromag-

netic field. In the whispering gallery modes, light circulates around the curved inner boundary of the resonator, reflecting from the walls of the resonator. This reflection always has an angle of incidence greater than the critical angle, to ensure the total internal reflection. Thus light remains trapped inside the resonator. There are only small losses of light caused by evanescent leakage and scattering from surface roughness. The whispering gallery modes can thus be related to the whispering gallery motion as discusses in this paper for the circular and elliptical billiard system.

The evanescent light escape in this micro-disk lasers is thus by tunneling. This preserves the rotational symmetry of the system, giving rise to a uniform light output in all directions. This however is not yet a useful laser, because the characteristic directionality of light emission is missing. To account for this fact, one can look at the domain of chaos. In order to obtain a suitable modulation of the laser's far field [4], one has to break the rotational symmetry, i.e. deform the circular shape of the resonator. These systems are then called chaotic micro-lasers. To achieve this, very little deformation suffices in order to drastically change the far field, as can be seen at the bottom of Figure 10. This causes the resonator shape to be still rather circular, thus light still can be confined in the whispering gallery modes. However, the rotational symmetry is sufficiently broken such that one can obtain a reasonable directional far-field emission from such modes.

Knowing that the defining property of a laser is coherent light emission in a certain direction, the question arises how one can fulfill this requirement with a chaotic micro-disk laser. Chaotic implies that the far-field characteristics are sensitive to the slightest changes in the shape of the micro-cavity. At this point, let one look back at what was discusses previously, chaotic micro-disk lasers as billiards for light. Since the light is confined by total internal reflection as long as the angle of incidence is larger than a certain critical angle. But for smaller angles of incidence, the light is at least partially transmitted outside the micro-laser according to Fresnel's laws. As discussed before in this paper, for the circular and elliptical billiard systems, the angle of incidence is conserved in circular micro-lasers. However, this varies in chaotic micro-cavities. If we start a light ray starts well above the critical angle, at one point its angle of incidence will drop below, and thus the light ray can then refractively escape. When perturbed whispering gallery mode, the refractive escape will occur likely at boundary regions with higher curvature [7].

The far-field characteristics of the chaotic micro-lasers are mostly determined by how the light rays cross from the case of total internal reflection to the case of refractive escape, which is also called the critical line. In the field of dynamical systems, this is called an unstable manifold, the collection of all unstable directions of the billiard systems. The micro-disk laser can be seen as a Hamiltonian system with two degrees of freedom, where its configuration space is spanned by the arc length position along the boundary and the angle of incidence for each reflection. For each point in this phase space, one can find a stable and an unstable direction. The original shape of this point cloud will very soon be deformed and develop filaments. This

has to happen because without the expanding direction there would be no chaos, and a contracting direction is then needed to fulfill Liouville's theorem [1]. This will be the unstable direction, i.e. the one in which the filaments grow such that they eventually cross the critical line, which determines the far-field characteristics of the micro-laser.

This fact explains the robustness of the far field. If one has an individual light ray, it will react very sensitively to the slightest changes in the resonator shape since the system is chaotic. However, the unstable manifold sort of averages over, and their filaments remain rather robust. The characteristics of the far-field can be optimized via the unstable manifold by varying the resonator shape.

Until now the explanation was done with the use of light rays, but light can also be seen as a wave. This however is not a problem, as ray simulations agree remarkably well both with experimental data and wave simulations. This is a nice example of the power of the concept of ray-wave correspondence. The agreement between the far fields obtained from wave computations and ray simulations, and the experimental results can be seen in Figure 11 for the case of Limaçon-shaped micro-disk lasers [4].

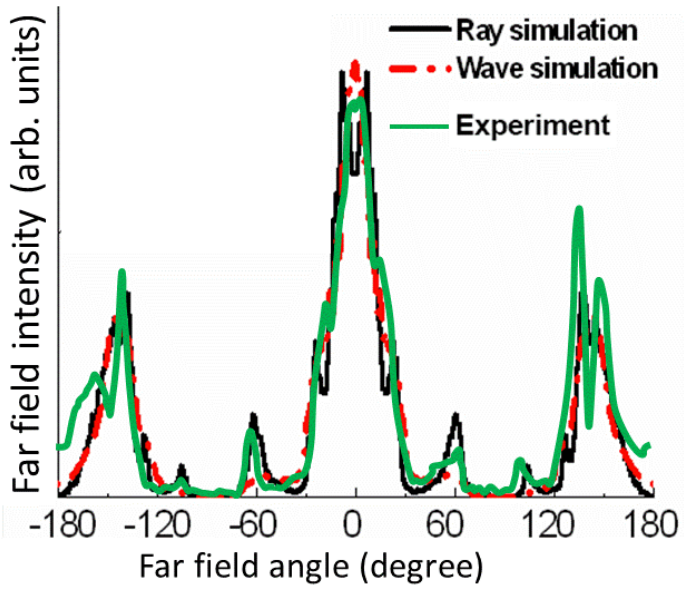

Figure 11: Far-field emission pattern of Limaçon-shaped micro-lasers.

Examples of the use of chaotic micro-lasers are quantum mechanics of electrons that are confined in asymmetric "boxes", such as quantum-dots, stadia, and quantum corrals. Furthermore, one can look at the asymmetric microwave cavities with their strong connection to quantum chaos theory. Looking at future applications, micro-lasers have possible applications in optical computing and networking. However, they are also of strong interest in research problems of cavity quantum electrodynamics, such as resonator-enhanced spontaneous emission and threshold-less lasers [16]. They may also serve as model systems for the study of wave phenomena in mesoscopic systems, particularly in the regime where motion is fully or partially chaotic.

5 Conclusion

In the first part of the paper, the general notion of billiard systems was explained, together with the existence of caustics in these systems. The mean minimal action function α was introduced and discussed in some detail. Furthermore, an example of a circular billiard was given.

The second part of the paper covered the derivation of the mean minimal action function α for the case of the elliptical billiard system. This was done by first introducing the billiard family, denoting the Hamiltonian of the system, and using this to find the actions and winding number. Then these results were used to derive α and it was compared to the circular case.

The last part of the paper was about an application of the results from the first two parts, the chaotic micro-lasers. The concept of micro-lasers was explained, what they are and where they are used, and then the physics of the chaotic micro-lasers was discussed in detail. At the end, the connection of micro-lasers to the billiard systems was looked at.

It can be said that the main goal of my research was completed. I learned more about the billiard systems, what they are, and where they are used. I also learned what the mean minimal action of these systems are, and how this relates to other fields of study. First I used this knowledge to work out the case of a circular billiard, and then used this knowledge to work out the more complicated case of the elliptical billiards. At the end, I was able to find the mean minimal action for these elliptical billiards and compared it with the circular case. To finish off the research it was interesting to see that billiard systems are even related to something like lasers, and to find out how they work and where they are and can be used.

References

[1] Arnold, V., Vogtmann, K. and Weinstein, A., 2013. *Mathematical Methods Of Classical Mechanics*. New York, NY: Springer.

[2] Biryuk, A. and Gomes, D., 2010. *An introduction to the Aubry-Mather theory*. The São Paulo Journal of Mathematical Sciences, 4(1), p.17.

[3] Gmachl, C., 1998. *High-Power Directional Emission from Microlasers with Chaotic Resonators*. Science, 280(5369), pp.1556-1564.

[4] Hentschel, M., 2015. *Chaotic microlasers*. Scholarpedia, 10(9), p.30923.

[5] Lazutkin, V., 1973. *THE EXISTENCE OF CAUSTICS FOR A BILLIARD PROBLEM IN A CONVEX DOMAIN*. Mathematics of the USSR-Izvestiya, 7(1), pp.185-214.

[6] Mather, J., 1990. *Differentiability of the minimal average action as a function of the rotation number*. Boletim da Sociedade Brasileira de Matemática, 21(1), pp.59-70.

[7] Nöckel, J. and Stone, A., 1997. *Ray and wave chaos in asymmetric resonant optical cavities*. Nature, 385(6611), pp.45-47.

[8] Poritsky, H., 1950. *The Billard Ball Problem on a Table With a Convex Boundary–An Illustrative Dynamical Problem*. The Annals of Mathematics, 51(2), p.446.

[9] Rayleigh, Lord, 1878. *Theory Of Sound*. 1st ed. London: Macmillan.

[10] Richter, P., Wittek, A., Kharlamov, M. and Kharlamov, A., 1995. *Action Integrals for Ellipsoidal Billiards*. Zeitschrift für Naturforschung A, 50(8).

[11] Siburg, K. F., 1999. *Aubry-Mather Theory and the Inverse Spectral Problem for Planar Convex Domains*. Israel Journal of Mathematics, 113, pp.285-304.

[12] Stöckmann, H., 2006. *Quantum Chaos*. Cambridge: Cambridge University Press.

[13] Stone, A., 2010. *Chaotic billiard lasers*. Nature, 465(7299), pp.696-697.

[14] Tabachnikov, S., 2009. *Geometry And Billiards*. Providence, RI: American Mathematical Soc.

[15] Waalkens, H., Wiersig, J. and Dullin, H., 1997. *Elliptic Quantum Billiard*. Annals of Physics, 260, pp.50-90.

[16] Yokoyama, H. and Ujihara, K., 1995. *Spontaneous Emission And Laser Oscillation In Microcavities*. Boca Raton: CRC Press.